 FDMP, vol.8, no.1, pp.69-90, 2011

Effect of a Porous Layer on the Flow Structure and Heat Transfer in a Square Cavity

S. Hamimid[1], M. Guellal[1], A. Amroune[1] and N. Zeraibi[2]

Abstract: A two-dimensional rectangular enclosure containing a binary-fluid saturated porous layer of finite thickness placed in the centre of the cavity is considered. Phase change is neglected. Vertical and horizontal solid boundaries are assumed to be isothermal and adiabatic, respectively. A horizontal temperature gradient is imposed, driving convection of buoyancy nature. The Darcy equation, including Brinkman and Forchheimer terms is used to account for viscous and inertia effects in the momentum equation, respectively. The problem is then solved numerically in the framework of a Velocity-Pressure formulation resorting to a finite volume method based on the standard SIMPLER algorithm. The effects of the governing parameters (geometric, hydrodynamic and thermal) on fluid flow and heat transfer are investigated.

Nomenclature

A	aspect ratio,
Cp	specific heat at constant pressure, $J.kg^{-1}.k^{-1}$
Da	Darcy number, $K.H^{-2}$
g	gravitational acceleration , $m.s^{-2}$
H	height of the enclosure, m
k	thermal conductivity, $W.m^{-1}.K^{-1}$
K	Permeability, m^2
L	width of the enclosure, m
Nu	Nusselt number
Nu_{avg}	average Nusselt number
p	fluid pressure , Pa
P	dimensionless pressure,
Pr	Prandtl number, $\Pr = \nu/\alpha$.
Ra	Rayleigh number, $Ra = \frac{g\beta\Delta TL^3}{\nu\alpha}$

[1] L.G.P.C. UFA-SETIF, Algeria
[2] UMBB, Boumerdes, Algeria

t	time, s
T	dimensional temperature, K
$T_C(T_H)$	temperature on left (right) vertical wall of cavity, $T_h \succ T_c$,K
T_0	reference temperature $T_0 = \frac{T_C - T_H}{2}, K$
u	velocity in x-direction , $m.s^{-1}$
v	velocity in y-direction , $m.s^{-1}$
$\overrightarrow{V}$	field velocity $(u\overrightarrow{ex} + v\overrightarrow{ey})$, $m.s^{-1}$
x,y	cartesian coordinates , m
X, Y	dimensionless coordinates
XP	dimensional width of the porous layer, m
Xp	dimensionless width of the porous layer, $XP.L^{-1}$

Greek symbols

α	Thermal diffusivity, $m^2.s^{-1}$
β	thermal expansion coefficient: $k^{-1}, -1/\rho_0(\partial\rho/\partial T)$
ρ	fluid density, $Kg.m^{-3}$
μ	dynamic viscosity of the fluid, $Kg.m^{-1}.s^{-1}$
ν	kinematic viscosity, $m^2.s^{-1}$
ΔT	temperature difference, $\Delta T = T_C - T_F$, K
ε	porosity of the porous layer
Ψ	stream function: $u = -\partial\psi/\partial y$; $v = \partial\psi/\partial x$, $m^2.s^{-1}$
θ	dimensionless temperature, $\theta = \frac{T - T_0}{\Delta T}$
τ	dimensionless time
σ	ratio of heat capacities $\left(\left\{\varepsilon(\rho c_p)_f + (1-\varepsilon)(\rho c_p)_s\right\}/(\rho c_p)_f\right)$

Subscripts

eff	effective property of the porous layer
max	maximum value
min	minimum value
avg	average value
0	reference state
C	cold
H	hot
f	refers to the fluid domain
s	refers to the porous medium

1 Introduction

Thermally driven flows in porous media have received a great deal of attention, this being due to a large number of technical applications and because of the increasing interest in engineering applications such as, fluid flow in geothermal reservoirs, geothermal energy systems, compact heat exchangers, separation processes in chemical industries, dispersion of chemical contaminants through water saturated soil, solidification of casting, migration of moisture in grain storage system, crude oil production, nuclear engineering, cooling of radioactive waste containers etc. A detailed review of the topic has been given by Nield and Bejan (2006).

Despite the absence of experimental work and a lack of practical applications, several theoretical papers, including those by Patil and Rudraiah (1973), Muthtamilselvan and Kandaswamy (2009) and Rudraiah (1984), have been published on magnetohydrodynamic convection in a horizontal layer. The simplest case is that of an applied vertical magnetic field and electrically conducting boundaries.

Recently the combined effect of mixed convection with thermal radiation and chemical reaction on MHD flow of viscous and electrically conducting fluid past a vertical permeable surface embedded in a porous medium have been investigated by Pal and Talukdar (2010). The results obtained show that the velocity, temperature and concentration fields are appreciably influenced by the presence of chemical reaction, thermal stratification and magnetic field. It is observed that the effect of thermal radiation and magnetic field is to decrease the velocity, temperature and concentration profiles in the boundary layer. There is also considerable effect of magnetic field and chemical reaction on skin-friction coefficient and Nusselt number.

Robillard *et al.* (2006) investigated numerically as well as analytically the effect of an electromagnetic field on the natural convection in a vertical rectangular porous cavity saturated with an electrically conducting binary mixture. They conclude that under the condition of constant fluxes of heat and mass imposed at the long side walls of the layer, the flow is parallel in the core of the cavity and turns through 180° in regions close to the end boundaries. This flow structure is not affected by the imposition of a magnetic field.

The effect of porosity on natural convective flow and heat transfer in fluid saturated porous medium has been investigated using Galerkin's finite element method by Nithiarasu, Seetharamu and Sundararajan (1998a). A generalised non-Darcy flow model with porosity as a separate parameter was used. Results indicate that the non-Darcy regime is highly sensitive to porosity changes. A variation of order of 40% in the average Nusselt number was possible with change in the porosity, for the Rayleigh and Darcy number ranges considered.

Straughan (2010) examined how the structure of the Darcy and Forchheimer coefficients (as functions of the porosity) might influence flows in porous media; it was proved that the flow solution in a Forchheimer porous material depends continuously on changes in the porosity.

Convection in a fluid-filled square cavity with differentially heated vertical walls covered by thin porous layers was studied numerically by Le Breton *et al*. (1991). They showed that porous layers having a thickness of the order of the boundary layer thickness were sufficient to reduce the overall Nusselt number significantly (by an amount that increased with the increase of Ra) and thicker porous layers produced only a small additional decrease in heat transfer.

Many studies have been recently devoted to double diffusive natural convection in binary mixtures confined in enclosures [Gobin and Goyeau (2005); Goyeau and Gobin (1999); Bennacer and Beji (2003); Mharzi et al. (2000)].

The study of Goyeau and Gobin (1999), in particular, was focused on the influence of the porous layer permeability on the overall heat transfer. The numerical results showed that the convective flow structure, and consequently the heat transfer, results from a complex interaction between the viscous drag in the porous layer and the driving force enhancement due to the flow penetration.

A two-dimensional mathematical model based on Darcy's law with Boussinesq approximation was used by Alavyoon and Masuda (1994) to study double-diffusive natural convection in a rectangular fluid-saturated vertical porous enclosure subject to opposing and horizontal gradients of heat and solute.

Combined heat and mass transfer process by natural convection along a vertical wavy surface in a thermal and mass stratified fluid saturated porous enclosure has been numerically analysed by Kumar and Shalini (2005). The finite element method was used and the influence of varying flow, heat and mass transfer governing parameters was reported. Presence of thermal and mass stratification terms was found to reduce the Nusselt number and Sherwood number values in all cases.

Singh and Thorpe (1995) presented a comparative study of the Darcy, Brinkman-extended Darcy and Brinkman-Forchheimer-extended Darcy models of free convection in a cavity containing a fluid layer overlying a porous layer saturated with the same fluid. The two-dimensional enclosure was heated on one vertical side and cooled at the opposite side, while the top and bottom sides were adiabatic.

A non-similar boundary-layer analysis was performed by Mahdy (2010), who considered the flow, heat and mass transfer characteristics of non-Darcian mixed convection of a non-Newtonian fluid originating from a vertical isothermal plate embedded in a homogeneous porous medium with the Soret and Dufour effects and in the presence of either surface injection or suction. The considered value of the

mixed-convection parameter was between 0 and 1. In addition, a power-law model was used for non-Newtonian fluids with exponent n < 1 for pseudoplastics n = 1 for Newtonian fluids and n > 1 for dilatant fluids.

By using the mathematical formalism of absolute and convective instabilities Hirata, Najib and Ouarzazi (2010) investigated the nature of unstable three-dimensional disturbances of viscoelastic flow convection in a porous medium with horizontal through-flow and a vertical temperature gradient. Temporal stability analysis revealed that among three-dimensional ($3D$) modes the pure down-stream transverse rolls are favored for the onset of convection. In addition, by considering a spatiotemporal stability approach they found that all unstable $3D$ modes were convectively unstable except the transverse rolls (which were observed to experience a transition to absolute instability).

The influence of the heat transfer at free surface (represented by Biot number) on the Rayleigh-Marangoni-Bénard instability in a system represented by coupled liquid–porous layers with top free surface was investigated numerically by Zhao and Liu (2010).

Other relevant studies are due to Bennamoun and Belhamri (2008), Henda et al. (2008), El Alami et al. (2009), Bucchignani (2009), Aouachria (2009), Djebali et al. (2009), Mezrhab and Naji (2009), Mechighel et al. (2009), Plappally et al. (2009), Podolny et al. (2010), Bataller (2010), Rouijaa et al. (2011), Abbassi et al. (2011), Meskini et al. (2011).

In the present study, in particular, attention is given to the overall heat transfer and fluid flow occurring inside a square cavity that is separated in two fluid filled regions by a fluid saturated porous medium. The interface between the fluid and the porous medium is permeable, and the flow in the porous layer is modelled using the Darcy-Brinkman-Forchheimer extended law (to account for no-slip on the walls and on the fluid/porous interfaces). The considered fluid is air (Pr = 0.71). The effects of the dimensionless groups, Rayleigh, Ra, Darcy, Da, numbers are examined.

2 Physical model and governing equations

The domain under consideration is a two-dimensional rectangular enclosure (width L, height H, aspect ratio A = H/L) containing a fluid saturated porous layer of finite thickness XP placed in the centre of the cavity, and bounded by two vertical fluid layers of equal width. The vertical surfaces are kept at constant temperature T_C (at x = 0) and T_H (at x = L) such that $T_H > T_C$ thus giving rise to the phenomenon of free convection within the cavity. The horizontal walls are considered to be adiabatic (zero normal temperature gradients are imposed at the horizontal surfaces).

The composite fluid/porous system, boundary conditions and the coordinate system

for the problem under consideration are depicted in Fig.1.

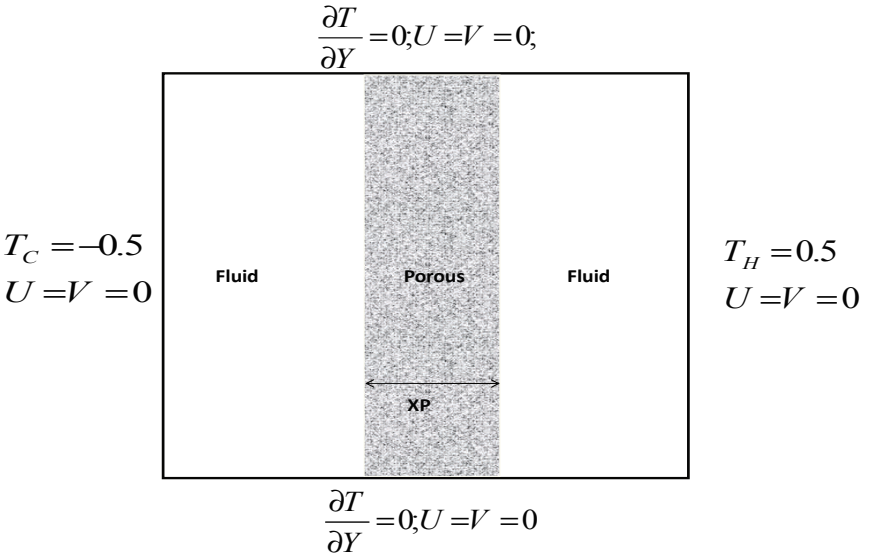

Figure 1: Schematic representation of the cavity.

The porous medium is completely saturated with the fluid and is assumed to be macroscopically isotropic, homogeneous and in local thermal equilibrium.

The fluid is assumed to satisfy the classical hypotheses for an incompressible Newtonian fluid. The Boussinesq approximation is satisfied, assuming that the fluid density is a constant, except in the driving term of the momentum equation where it varies linearly with both temperature.

$$\rho(T)=\rho_0[1-\beta_T(T-T_0)] \tag{1}$$

Where: $\beta_T=-\frac{1}{\rho_0}(\frac{\partial\rho}{\partial T})_P$.

Also, the Darcy-Brinkman-Forchheimer model is used in the momentum equation.

Fluid Region

$$\frac{\partial u}{\partial x}+\frac{\partial v}{\partial y}=0 \tag{2}$$

$$\rho\left(\frac{\partial u}{\partial t}+u\frac{\partial u}{\partial x}+v\frac{\partial u}{\partial y}\right)=-\frac{\partial P}{\partial x}+\mu(\frac{\partial^2 u}{\partial x^2}+\frac{\partial^2 u}{\partial y^2}) \tag{3}$$

$$\rho\left(\frac{\partial v}{\partial t}+u\frac{\partial v}{\partial x}+v\frac{\partial v}{\partial y}\right)=-\frac{\partial P}{\partial y}+\mu(\frac{\partial^2 v}{\partial x^2}+\frac{\partial^2 v}{\partial y^2})-\rho_{ref}g \tag{4}$$

$$\rho\ C_p\frac{\partial T}{\partial t}+\rho\ C_p(u\frac{\partial T}{\partial x}+v\frac{\partial T}{\partial y})=k(\frac{\partial^2 T}{\partial x^2}+\frac{\partial^2 T}{\partial y^2}) \tag{5}$$

With the assumption of Boussinesq : $\rho_{ref}=\rho-\rho_0=-\beta_t\,(T-T_0)$

Porous region

$$\frac{\partial u}{\partial x}+\frac{\partial v}{\partial y}=0 \tag{6}$$

$$\frac{1}{\varepsilon}\frac{\partial u}{\partial t}+\frac{1}{\varepsilon^2}u\frac{\partial u}{\partial x}+\frac{1}{\varepsilon^2}v\frac{\partial u}{\partial y}=-\frac{1}{\rho}\frac{\partial p}{\partial x}+\frac{\mu_{eff}}{\rho\varepsilon}\nabla^2 u-D_x \tag{7}$$

$$\frac{1}{\varepsilon}\frac{\partial v}{\partial t}+\frac{1}{\varepsilon^2}u\frac{\partial v}{\partial x}+\frac{1}{\varepsilon^2}v\frac{\partial v}{\partial y}=-\frac{1}{\rho}\frac{\partial p}{\partial y}+\frac{\mu_{eff}}{\rho\varepsilon}\nabla^2 v+\beta_t\,(T-T_0)\,g-D_y \tag{8}$$

$$(\rho\ C_p)_{eff}\frac{\partial T}{\partial t}+(\rho\ C_p)_f(u\frac{\partial T}{\partial x}+v\frac{\partial T}{\partial y})=k_{eff}(\frac{\partial^2 T}{\partial x^2}+\frac{\partial^2 T}{\partial y^2}) \tag{9}$$

$$(\rho\ C_p)_{eff}=\varepsilon.(\rho\ C_p)_f+(1-\varepsilon)\,(\rho\ C_p)_s \tag{10}$$

$$\left|\overline{V}\right|=\sqrt{u^2+v^2} \tag{11}$$

WhereD_x (D_y), is the matrix drag per unit volume of the porous medium in x- (y-) direction.

Turning our attention to the solid matrix drag per unit volume, it can be taken in the form:

$$D=AV+BV^2 \tag{12}$$

For a one-dimensional flow with velocity V, the above form of drag expression is supported by a variety of packed bed and fluidized bed correlations, including the widely used Ergun's (1952) correlation.

For a two-dimensional flow, the x- (y-) direction solid matrix drag contribution can be shown to be of the form :

$$D_x=Au+B(u^2+v^2)^{1/2}u \tag{13}$$

$$D_y=Av+B(u^2+v^2)^{1/2}v \tag{14}$$

By resolving, the vectorial drag expression along the y direction.

In the present work, we consider the Ergun's correlation with constants A and B given by :

$$A = 150\frac{(1-\varepsilon^2)}{\varepsilon^3}\frac{\mu_f}{D_p^2}$$
$$B = 1.75\frac{(1-\varepsilon^2)}{\varepsilon^3}\frac{\rho_f}{D_p} \tag{15}$$

It should be noted, however, that suitable correlations may be employed in different ranges of the bed porosity ε to obtain the non-Darcian flow behaviour inside the porous medium for a general simulation.

The above solid matrix drag relation can also be expressed in terms of the medium permeability K by defining:

$$K = \frac{\varepsilon^3 D_p^2}{150(1-\varepsilon)^2} \tag{16}$$

Now the solid matrix drag component D_x, D_y, can be written as :

$$D_x = \frac{\mu_f \overline{u}}{k} + \frac{1.75}{\sqrt{150}}\frac{\rho_f}{\sqrt{k}}\frac{|\overline{v}|}{\varepsilon^{3/2}}\overline{u} \tag{17}$$

$$D_y = \frac{\mu_f \overline{v}}{k} + \frac{1.75}{\sqrt{150}}\frac{\rho_f}{\sqrt{k}}\frac{|\overline{v}|}{\varepsilon^{3/2}}\overline{v} \tag{18}$$

The effective properties of the porous medium (subscript *eff)* are usually a complex function of the porosity and tortuosity of the solid matrix as well as of the local fluid velocity. In the following simulations, the interest is not focused on the influence of these parameters, and for the sake of simplicity, the corresponding fluid properties are used throughout the study.

$$\frac{1}{\varepsilon}\frac{\partial u}{\partial t} + \frac{1}{\varepsilon^2}u\frac{\partial u}{\partial x} + \frac{1}{\varepsilon^2}v\frac{\partial u}{\partial y} = -\frac{1}{\rho}\frac{\partial p}{\partial x} + \frac{\mu_{eff}}{\rho\varepsilon}\nabla^2 u - \frac{\mu_{eff}}{\rho k}u - \frac{1.75}{\sqrt{150}}\frac{1}{\sqrt{k}}\frac{\left|\overline{V}\right|}{\varepsilon^{3/2}}u \tag{19}$$

$$\frac{1}{\varepsilon}\frac{\partial v}{\partial t} + \frac{1}{\varepsilon^2}u\frac{\partial v}{\partial x} + \frac{1}{\varepsilon^2}v\frac{\partial v}{\partial y} = -\frac{1}{\rho}\frac{\partial p}{\partial y} + \frac{\mu_{eff}}{\rho\varepsilon}\nabla^2 v + \beta_t\left(T - T_0\right)g - \frac{\mu_{eff}}{\rho k}v - \frac{1.75}{\sqrt{150}}\frac{1}{\sqrt{k}}\frac{\left|\overline{V}\right|}{\varepsilon^{3/2}}v \tag{20}$$

$$(\rho\, C_p)_{eff}\frac{\partial T}{\partial t} + (\rho\, C_p)_f\left(u\frac{\partial T}{\partial x} + v\frac{\partial T}{\partial y}\right) = k_{eff}\left(\frac{\partial^2 T}{\partial x^2} + \frac{\partial^2 T}{\partial y^2}\right) \tag{21}$$

$$(\rho\, C_p)_{eff} = \varepsilon.(\rho\, C_p)_f + (1-\varepsilon)(\rho\, C_p)_s \tag{22}$$

In view of the foregoing description, and using the following change of variables:

$$\tau = \frac{t}{H^2/\alpha}, \quad X = \frac{x}{H}, \quad Y = \frac{y}{H}, \quad U = \frac{uH}{\alpha}, \quad V = \frac{vH}{\alpha}$$

$$P = \frac{\varepsilon^2 pH^2}{\rho\alpha^2}, \quad \theta = \frac{T - T_0}{\Delta T},$$

$$\Delta T = T_H - T_C, \quad T_0 = \frac{T_H + T_C}{2}$$

The governing equations for unsteady two-dimensional natural convection flow in the porous cavity using conservation of mass, momentum and energy may be written as follows:

Fluid Region

$$\frac{\partial U}{\partial X} + \frac{\partial V}{\partial Y} = 0 \tag{23}$$

$$\frac{\partial U}{\partial \tau} + U\frac{\partial U}{\partial X} + V\frac{\partial U}{\partial Y} = -\frac{\partial P}{\partial X} + \mathrm{Pr}\,\nabla^2 U \tag{24}$$

$$\frac{\partial V}{\partial \tau} + U\frac{\partial V}{\partial X} + V\frac{\partial V}{\partial Y} = -\frac{\partial P}{\partial Y} + \mathrm{Pr}\,\nabla^2 V + Ra\,\mathrm{Pr}\,\theta \tag{25}$$

$$\frac{\partial \theta}{\partial \tau} + \left(U\frac{\partial \theta}{\partial X} + V'\frac{\partial \theta}{\partial Y}\right) = \left(\frac{\partial^2 \theta}{\partial X^2} + \frac{\partial^2 \theta}{\partial Y^2}\right) \tag{26}$$

Porous region

$$\frac{\partial U}{\partial X} + \frac{\partial V}{\partial Y} = 0 \tag{27}$$

$$\varepsilon\frac{\partial U}{\partial \tau} + U\frac{\partial U}{\partial X} + V\frac{\partial U}{\partial Y} = -\frac{\partial P}{\partial X} + \mathrm{Pr}\,\varepsilon\nabla^2 U - \frac{\mathrm{Pr}}{Da}\varepsilon^2 U - \frac{1.75}{\sqrt{150}}\frac{\varepsilon^{1/2}}{\sqrt{Da}}\left|\sqrt{U^2+V^2}\right| U \tag{28}$$

$$\varepsilon\frac{\partial V}{\partial \tau} + U\frac{\partial V}{\partial X} + V\frac{\partial V}{\partial Y} = -\frac{\partial P}{\partial Y} + \mathrm{Pr}\,\varepsilon\nabla^2 V + Ra\,\mathrm{Pr}\,\varepsilon^2\theta - \frac{\mathrm{Pr}}{Da}\varepsilon^2 V - \frac{1.75}{\sqrt{150}}\frac{\varepsilon^{1/2}}{\sqrt{Da}}\left|\sqrt{U^2+V^2}\right| V \tag{29}$$

$$\sigma\frac{\partial\theta}{\partial\tau}+\left(U\frac{\partial\theta}{\partial X}+V\frac{\partial\theta}{\partial Y}\right)=\left(\frac{\partial^2\theta}{\partial X^2}+\frac{\partial^2\theta}{\partial Y^2}\right) \tag{30}$$

With the initial and boundary conditions

$U=V=0, \quad \theta = \theta_i$ for $\tau=0$

$U=V=0, \quad \theta=\theta_C=-0.5$ for $0\le Y\le H$ at $X=0$

$U=V=0, \quad \theta=\theta_H=0.5$ for $0\le Y\le H$ at $X=L$

$U=V=0, \quad \frac{\partial\theta}{\partial Y}=0$ for $0\le X\le L$ at $Y=0$

$U=V=0, \quad \frac{\partial\theta}{\partial Y}=0$ for $0\le X\le L$ at $Y=H$

3 Method of solution

The governing equations along with the boundary conditions are solved numerically using a finite volume method with a staggered grid arrangement. The conservation equations are integrated on the control volumes defined by the computational grid; a power scheme was also used in approximating advection–diffusion terms.

The fluid flow is unsteady, laminar and incompressible. The pressure work and viscous dissipation are all assumed negligible. The thermophysical properties of the porous medium are taken to be constant. However, the Boussinesq approximation takes into account of the effect of density variation on the buoyancy force.

Convergence of the numerical iterations is achieved when the local criterion

$$\max\left|\frac{\varphi^{m+1}-\varphi^m}{\varphi^m}\right| \prec 10^{-5} \tag{31}$$

is satisfied. In equation (31) φ represents all three main variables, U, V, P and θ, at every location of the discretized domain. The indexes m and m+1 are any two consecutive iterations at the same time τ.

Solution of linear algebraic equation is made by TDMA (Three Diagonal Matrix Algorithm). An under-relaxation parameter of 0.3, 0.3, 0.4 and 0.5 for Da$\le 10^{-5}$ and 0.7, 0.7, 0.7 and 0.9 for Da$\ge 10^{-4}$ were used in order to obtain a stable convergence for the solution of *u*-velocity, *v*-velocity, pressure and energy equations.

A grid sensitivity study shows that a non-uniform mesh of 80x80 is sufficient to carry out the computation. To ensure more accurate results, a non-uniform mesh of 100x100 has been employed in the present study.

The non-dimensional heat transfer rate in terms of local Nusselt number, *Nu*, from the right vertical heated surface is given by

$$Nu(Y)=-\left.\frac{\partial\theta(X,Y)}{\partial X}\right|_{X=L} \tag{32}$$

The corresponding value of the average Nusselt number, denoted by Nu_{avg}, may be calculated from the following relation

$$Nu_{av} = \frac{1}{H}\int_0^H Nu(y)dy = -\frac{1}{H}\int_0^H \left(\frac{\partial\theta(x,y)}{\partial x}\right)_{x=L} dy \tag{33}$$

4 Test Validation

The numerical accuracy of the present study has been checked over a large number of purely thermal - convection cases. The results are compared with earlier studies in Tables 1 and 2, for the Darcy and combined Darcy Brinkman representation of the porous medium flow. The validation has been performed using 120 x 120 non - uniform grids. It may be seen from the Tables, that the agreement with Lauriat and Prasad (1989) and Nithiarasu et al. (1998b) is excellent in most cases (indeed, our results present a difference less than 2% in comparison to Nithiarasu et al.).

Table 1: Darcy model

$Ra^* = Ra_t.Da$	Nu_{avg}		
	Lauriat and Prasad (1989)	Nithiarasu et al. (1998b)	Present work
10	1.07	1.08	1.121
50	n.d	1.958	1.961
100	3.09	3.02	3.120
500	n.d	8.38	8.411
1000	13.41	12.514	12.531

Table 2: Darcy - Brinkman model

$Ra^* = Ra_t.Da$	Da	Nu_{avg}		
		Lauriat and Prasad (1989)	Nithiarasu et al. (1998b)	Present work
10	10^{-6}	1.07	1.08	1.120
100	10^{-6}	3.06	3.00	3.118
1000	10^{-6}	13.2	12.25	12.205
10	10^{-2}	1.02	1.02	1.110
100	10^{-2}	1.7	1.71	1.732
1000	10^{-2}	4.26	4.26	4.253

5 Results and discussions

In the following, we restrict this study to a square cavity (A = 1) filled with air (Pr = 0.71) separated in two equal parts (x_1 = 0.4) by a saturated porous medium of dimensionless thickness X_P = 0.2. The Rayleigh number ranges from 10^3 to 10^7 and the Darcy number from 10^{-6} to 1.

5.1 Effect of Da and Ra on heat transfer and fluid flow

The influence of the permeability of the porous layer on the flow structure is illustrated by the streamlines plotted in fig. (6a, 9a), vertical V-velocity at mid height of the enclosure plotted in fig. (5a, 8a) and the maximum of the stream function plotted in fig.(2a), for different values of the Darcy number. The results are displayed for the two cases; $Ra = 10^7$ and 10^3 (for large and small buoyancy forces).

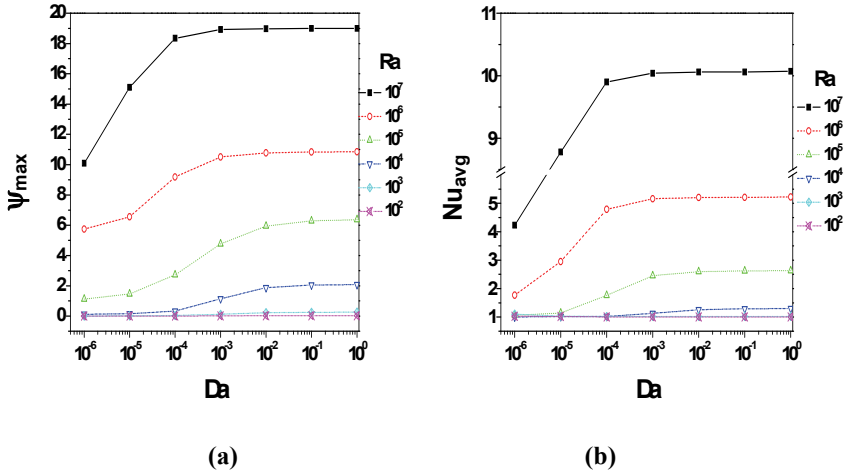

Figure 2: (a) Extremum of the stream function and (b) Average Nusselt number variation with Darcy number for different Rayleigh number values and for $XP = 0.2$, $\varepsilon = 0.4$.

Figures (5a,5b) illustrate the vertical velocity and temperature at mid height of the enclosure for $Ra = 10^7$. As depicted in this figure, the effect of increasing the value of porous permeability is to increase the value of the temperature and velocity components in the porous layer due to the fact that drag is reduced by increasing the value of the porous permeability on the fluid flow which results in increased velocity.

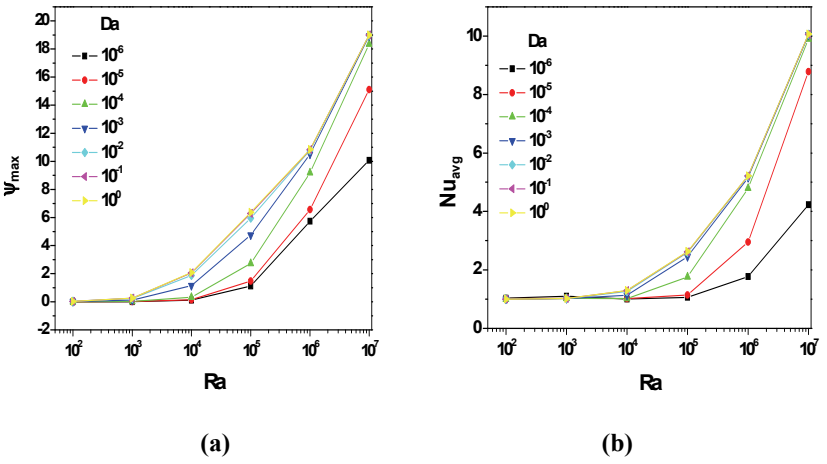

Figure 3: Infuence of Ra and Da on Nu_{avg} and $\psi_{\max}$ for $XP = 0.2$, $\varepsilon = 0.4$.

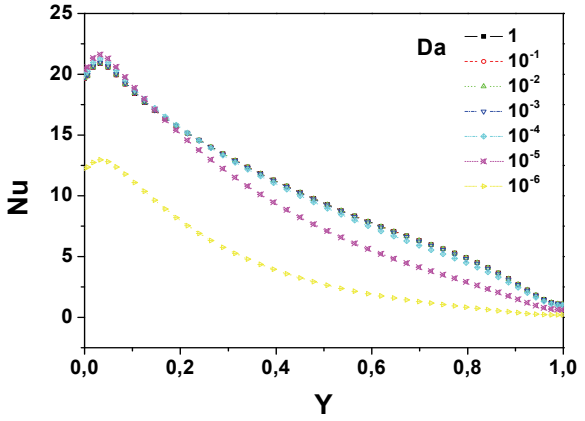

Figure 4: Local Nusselt number distribution on the right heated surface for different permeability of the porous layer *Da* and with, $Ra = 10^7$, $XP = 0.2$ and $\varepsilon = 0.4$.

At low Darcy numbers ($Da \leq 10^{-5}$), the porous layer behaves like a solid wall and becomes almost isothermal, fig. (6a,6b) and fig. (9a,9b). Then, with increasing permeability, the flow penetrates the porous domain and the corresponding heat transfer monotonously increases, fig. (2b) (Table 3); finally, for very high perme-

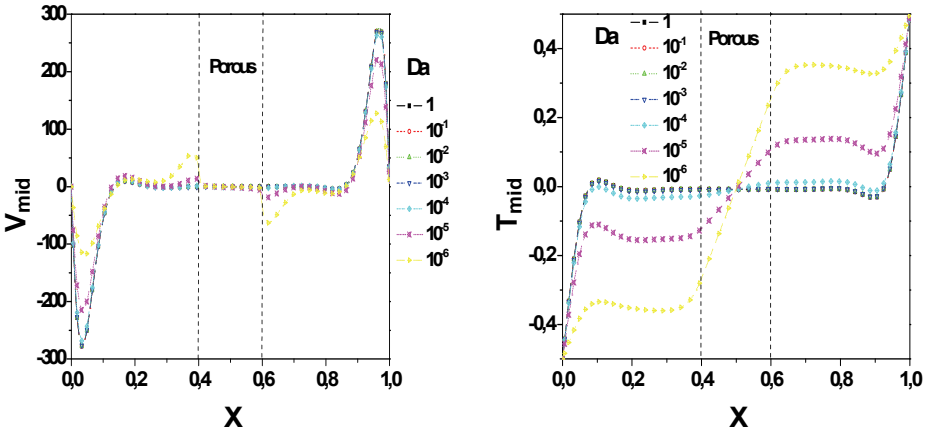

Figure 5: (a) V-velocity and (b) Temperature at mid height of the enclosure for $Ra = 10^7$, $XP = 0.2$ and $\varepsilon = 0.4$ and for different Darcy number.

abilities (Da > 10^{-4}), when the friction in the porous layer becomes negligible, the structure of streamlines and isotherms do not change much remaining the same for values of $Da > 10^{-3}$; correspondingly, the average Nusselt number, fig. (2b) (Table 3), reaches a constant value, corresponding to the solution for a fully fluid cavity. Obviously, these cases represent a gradual transition from conduction to convection in the porous region.

For relatively high values of the Rayleigh number (Ra$\geq 10^4$), it may also be noted that the relative increase of Nu_{avg} and the maximum of the stream function $\psi_{\max}$, fig. (2a, 2b) (Table 3), is significant at a lower values of Da (Da$\leq 10^{-4}$), whereas for a low buoyancy forces, (Ra$\leq 10^3$) the Nusselt number is not very sensitive to Da, tending to a constant value (Nu_{avg}=1) for Ra=10^3 (corresponding to the solution obtained for a fully fluid cavity).

Increasing simultaneously or separately Ra and Da favours the fluid to flow through the porous layer from one fluid region to the other, fig. (6a, 9a), so the intensities of natural convection flow and, consequently, local and average Nusselt numbers increase, fig. (2b) (Table 3), fig. 4. Moreover, the flow in the cavity is reduced when Ra and Da are made small, Fig. 3, especially for moderate Rayleigh numbers (Ra < 10^5). Accordingly, the fluid flow is confined in the fluid compartments, and the heat transfer in the porous layer occurs mainly by conduction [Beckermann et al. (1987)and 1988)].

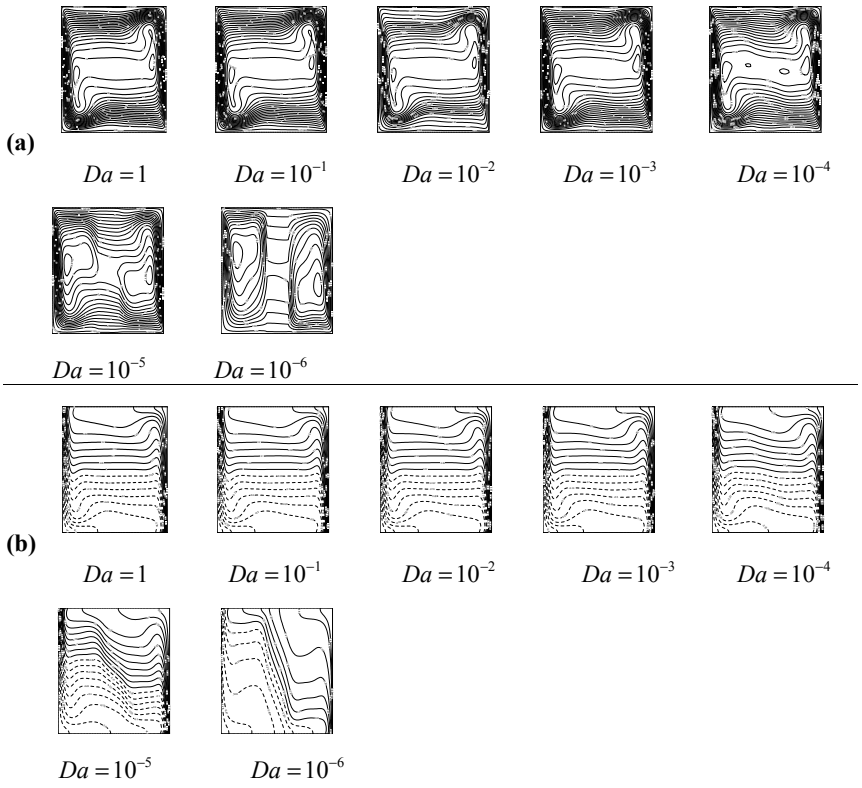

Figure 6: Streamlines (a) and isotherms (b) for $Ra = 10^7$, $XP = 0.2$ and $\varepsilon = 0.4$

The change in the fluid flow structure is accompanied with a change in the local Nusselt numbers curves, fig. 4 (the change becoming smaller as Da increases, especially for Da $\geq 10^{-4}$).

Figures 4 and fig. 7 show the effect of Darcy number Da on the local Nusselt number Nu(y) on the hot wall for various values of Rayleigh number Ra with $\varepsilon = 0.4$ and $XP = 0.2$. It can be clearly seen that the local Nusselt number for a large buoyancy force (Ra=10^7) tends to increase as the permeability of the porous layer increases, and from the values Da=10^{-4} the flow can be considered to be dominated by convection phenomenon, over the entire cavity. The local Nusselt number becomes almost independent of Da, and remains the same for values of *Da*> 10^{-4}.

For a small Ra (Ra=10^3), an increase in the Darcy number (Da$\geq 10^{-5}$) tends to

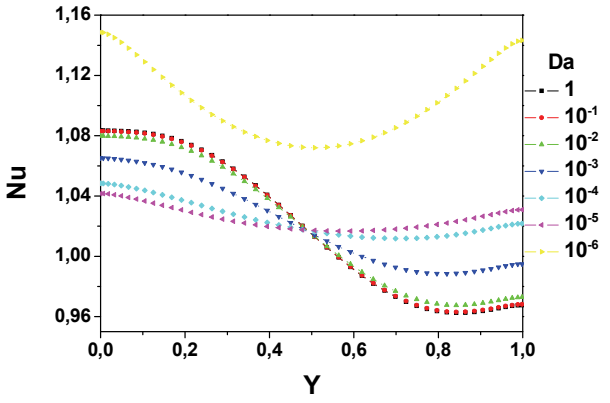

Figure 7: Local Nusselt number distribution on the right heated surface for different permeability of the porous layer Da and with, $Ra = 10^3$, $XP = 0.2$ and $\varepsilon = 0.4$

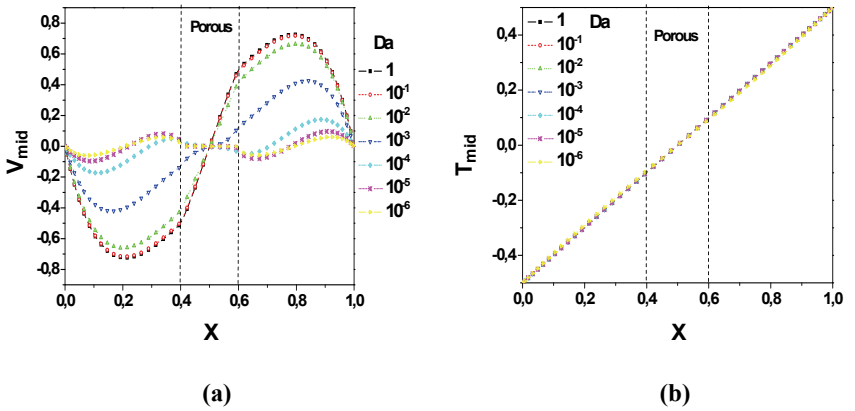

Figure 8: (a) V-velocity and (b) Temperature at mid height of the enclosure for Ra = 10^3, $XP = 0.2$and $\varepsilon = 0.4$ and for different Darcy number.

increase the local Nusselt number in the bottom part of the wall (y$\leq$0.5) and tends to decrease the local Nusselt number in the top part (y$\geq$0.5), but the evolution exhibits a minimum around y=0.5 for the value 10^{-6} of Darcy number.

In addition to this, it has been noted that the temperature distribution at the mid-height of the enclosure in the porous layer, fig. (5b), tend to become more linear for

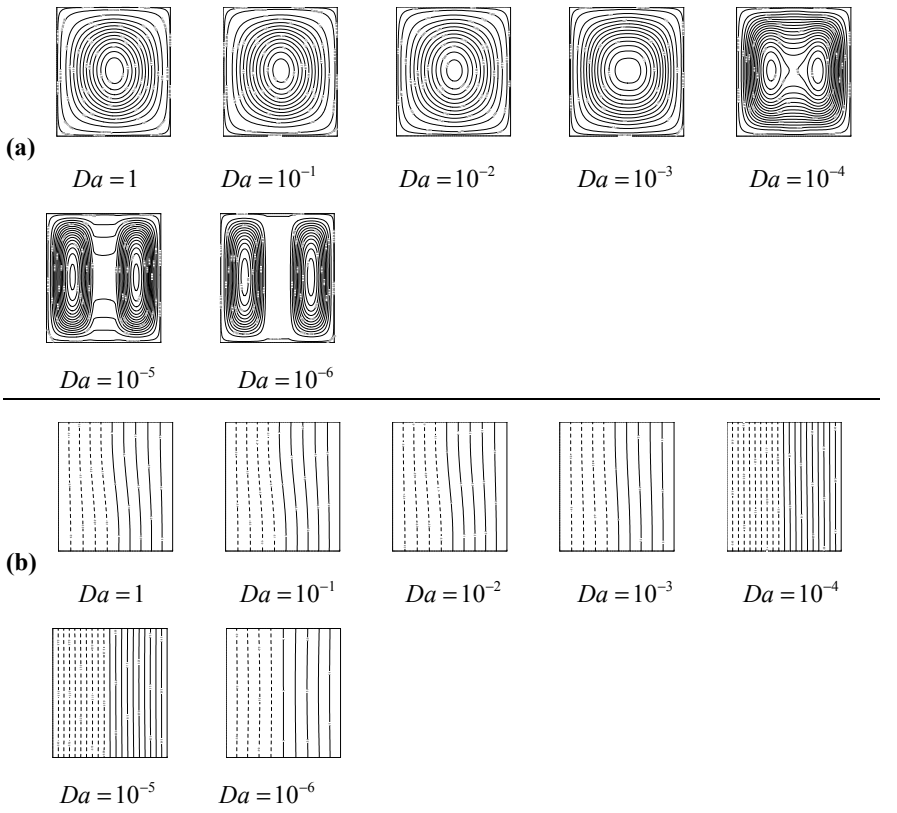

Figure 9: Streamlines (a) and isotherms (b) for different Darcy number for $Ra = 10^3$, $XP = 0.2$ and $\varepsilon = 0.4$.

a small Darcy number and at Ra =10^7, indicating that the heat transfer behavior deviates from the boundary layer and approaches the conduction limit, while thermal boundary layers appear at the vertical walls.

For a small Ra (Ra=10^3), the temperature profiles, fig. (8b), for each *Da* value vary linearly in the two regions, indicating that the heat transfer through the enclosure occurs mainly via conduction; the velocity profile, fig. (8a), for each *Da* value exhibits two maxima in the fluid regions for high and intermediate permeabilities (Da $\geq 10^{-3}$) around y=0.2 and y=0.8 and varies linearly in the porous region. Then with decreasing *Da,*(Da$\leq 10^{-4}$), the velocity component exhibits four maxima in the fluid regions around y =0.1 and y=0.3 in the left fluid region, and around y=0.7 and y=0.9 in the right fluid region and the porous layer is almost isothermal, fig.

(6b), fig. (9b).

Table 3: Extremum of the stream function and Average Nusselt number for Ra=10^2 to 10^7, Pr=0.7, XP=0.2, Da=1 to 10^{-6} and ε=0.4

	Da Ra	**1**	$\mathbf{10^{-1}}$	$\mathbf{10^{-2}}$	$\mathbf{10^{-3}}$	$\mathbf{10^{-4}}$	$\mathbf{10^{-5}}$	$\mathbf{10^{-6}}$
$\psi_{\max}$	10^7	19.0	19.0	18.98	18.93	18.35	15.11	10.08
	10^6	10.85	10.834	10.78	10.51	9.19	6.56	5.74
	10^5	6.37	6.29	5.95	4.76	2.73	1.47	1.12
	10^4	2.08	2.05	1.88	1.15	0.33	0.15	0.12
	10^3	0.257	0.254	0.23	0.124	0.032	0.014	0.008
	10^2	0.025	0.025	0.023	0.013	0.003	0.001	9e-4
Nu_{avg}	10^7	10.07	10.06	10.06	10.04	9.9	8.78	4.23
	10^6	5.22	5.21	5.20	5.16	4.79	2.95	1.77
	10^5	2.63	2.62	2.6	2.45	1.76	1.14	1.06
	10^4	1.3	1.29	1.26	1.13	1.02	1.017	1.00
	10^3	1.019	1.019	1.02	1.021	1.024	1.025	1.1
	10^2	1.00	1.00	1.00	1.00	1.00	1.02	1.03

6 Conclusions

Natural convection in vertical annular enclosures containing different amounts of porous insulation has been studied resorting to the Darcy model, including Brinkman and Forchheimer terms, to account for viscous and inertia effects, respectively, in the momentum equation.

The influence of the permeability of the porous layer on the average and local heat transfer characteristics in the enclosure has been assessed. The related numerical results lead to the main conclusion that the overall heat transfer increases with increasing permeability, this being due to a better penetration of the porous layer by the convective flow.

Moreover, according to the results, the thermal exchange is also sensitive to the Rayleigh number (the increase of Ra enhancing the convection in the fluid compartments of the cavity, with the convection in the porous layer being enhanced with the increase of Da).

In the region of larger Darcy numbers ($Da > 10^{-5}$), the effect related to the better penetration of the porous medium due to larger permeability, and the increase of the buoyancy forces due to larger effective temperature gradient across the layer combine to increase the flow intensity and the resulting overall Nusselt number. All the local indicators represented in Fig. (4, 5) and fig. (7, 8) (velocity components and

local heat transfer) grow with *Da* and reach a final value for infinite permeability corresponding to the ideal case in which the whole cavity is fluid.

These results are an important step toward a complete understanding the parameter space for convection heat transfer in composite systems.

References

Abbassi M.A., Halouani K., Chesneau X.; Zeghmati B. (2011): Combined Thermal Radiation and Laminar Mixed Convection in a Square Open Enclosure with Inlet and Outlet Ports, *FDMP: Fluid Dyn. Mater. Process*, vol. 7, no. 1, pp. 71-96.

Alavyoon, F.; Masuda, Y.; Kimura, Y. (1994): On natural convection in vertical porous enclosures due to opposing fluxes of heat and mass prescribed at the vertical walls, *Int. J. Heat Mass Transfer,* vol. 37, no. 2, pp. 195-206.

Aouachria Z. (2009): Heat and Mass Transfer Along of a Vertical Wall by Natural convection in Porous Media, *FDMP: Fluid Dyn. Mater. Process*., vol. 5, no. 2, pp. 137-148.

Bataller R.C., (2010), Towards a Numerical Benchmark for MHD Flows of Upper-Convected Maxwell (UCM) Fluids over a Porous Stretching Sheet, *FDMP: Fluid Dyn. Mater. Process*, vol. 6, no. 3, pp. 337-350.

Beckermann C.; Viskanta, R.; Ramadhyani, S. (1987): Natural convection flow and heat transfer between a fluid layer and a porous layer inside a rectangular enclosure, *J of Heat Transfer,* vol. 109, pp. 363-370.

Beckermann, C.; Viskanta, R.; Ramadhyani, S. (1988): Natural convection in vertical enclosures containing simultaneously fluid and porous layers, *J Fluid Mech,* vol. 186, pp. 257-284.

Bennacer, R.; Beji, H.; Mohamad, A.A. (2003): Double diffusive convection in a vertical enclosure inserted with two saturated porous layers confining a fluid layer, *International Journal of Thermal Sciences,* vol. 42, pp. 141–151.

Bennamoun L.; Belhamri A. (2008): Study of Heat and Mass Transfer in Porous Media: Application to Packed-Bed Drying, *FDMP: Fluid Dyn. Mater. Process*., vol. 4, no. 4, pp. 221-230.

Bucchignani E. (2009): An Implicit Unsteady Finite Volume Formulation for Natural Convection in a Square Cavity*, FDMP: Fluid Dyn. Mater. Process*., vol. 5, no. 1, pp. 37-60.

Djebali R., El Ganaoui M., Sammouda H.; Bennacer R., (2009): Some Benchmarks of a Side Wall Heated Cavity Using Lattice Boltzmann Approach*, FDMP: Fluid Dyn. Mater. Process,* vol. 5, no. 3, pp. 261-282.

El Alami M.; Semma E. A.; Najam M.; Boutarfa R. (2009): Numerical Study

of Convective Heat Transfer in a Horizontal Channel, *FDMP: Fluid Dyn. Mater. Process.*, vol. 5, no. 1, pp. 23-36.

Ergun, S. (1952): Fluid flow through packed columns, *Chemical Engineering Prcgress,* vol. 48, pp. 89-94.

Gobin, D.; Goyeau, B.; Neculae, A. (2005): Convective heat and solute transfer in partially porous cavities, *International Journal of Heat and Mass Transfer,* vol. 48, pp. 1898–1908.

Goyeau, B.; Gobin, D. (1999): Heat transfer by thermosolutal natural convection in a vertical composite Fluid-Porous cavity, *Int. Corant HeatMass Transfer,* vol. 26, no. 8, pp. 1115-1126.

Henda R.; Quesnel W.; Saghir Z. (2008): Analytical Solution of the Thermal Behavior of a Circulating Porous Heat Exchanger, *FDMP: Fluid Dyn. Mater. Process.*, vol. 4, no. 4, pp. 237-244.

Hirata, S. C.; Ouarzazi, M.N. (2010): Three-dimensional absolute and convective instabilities in mixed convection of a viscoelastic fluid through a porous medium, *Physics Letters* A , vol. 374, pp. 2661–2666.

Lauriat, G.; Prasad, V. (1989): Non-Darcian effects on natural convection in a square cavity with thin porous enclosure. *Int. J. Heat and Mass Transfer*, vol. 32, pp- 2135-2148.

Le Breton, P.; Caltagirone, J.P.; Arquis, E. (1991): Natural convection in a square cavity with thin porous layers on its vertical walls. *ASME J. Heat Transfer,* vol. 113, pp. 892–898.

Mahdy, A. (2010): Soret and Dufour effect on double diffusion mixed convection from a vertical surface in a porous medium saturated with a non-Newtonian fluid, *J. Non-Newtonian Fluid Mech.,* vol. 165, pp. 568–575.

Mechighel F., El Ganaoui M., Kadja M., Pateyron B.; Dost S. (2009): Numerical Simulation of Three Dimensional Low Prandtl Liquid Flow in a Parallelepiped Cavity Under an external Magnetic Field, *FDMP: Fluid Dyn. Mater. Process*, vol. 5, no. 4, pp. 313-330.

Meskini A., Najam M.; El Alami M., (2011), Convective Mixed Heat Transfer in a Square Cavity with Heated Rectangular Blocks and Submitted to a Vertical Forced Flow, *FDMP: Fluid Dyn. Mater. Process*, vol. 7, no. 1, pp. 97-110.

Mezrhab A.; Naji H. (2009), Coupling of Lattice Boltzmann Equation and Finite Volume Method to Simulate Heat Transfer in a Square Cavity, *FDMP: Fluid Dyn. Mater. Process*, vol. 5, no. 3, pp. 283-296.

Mharzi, M.; Daguenet, M.; Daoudi, S. (2000): Thermosolutal natural convection in a vertically layered fuid-porous medium heated from the side, *Energy Conver-*

sion & Management, vol. 41, pp. 1065-1090.

Muthtamilselvan, M. ; Kandaswamy, P.; Lee, J. (2009): Hydromagnetic Mixed Convection in a Lid-Driven Cavity Filled with a Fluid-Saturated Porous Medium, *Int. J. of Appl. Math. and Mech.*, vol. 5, no. 7, pp. 28-44.

Nield, D.A. ; Bejan, A.(2006): Convection in Porous Media, *third ed., Springer-Verlag, New York.*

Nithiarasu, P.; Seetharamu, K. N.; Sundararajan, T. (1998a): Effect of porosity on natural convective heat transfer in fluid saturated porous medium. *International Journal of Heat and Fluid Flow,* vol. 19, pp. 56-58.

Nithiarasu, P.; Seetharamu, K. N.; Sundararajan, T. (1998b): Double-diffusive natural convection in an enclosure filled with fluid-saturated porous medium: a generalized non-Darcy approach. *Numerical Heat Transfer*, Part A, vol. 30, pp. 413-426.

Pal, D.; Talukdar, B., (2010) Buoyancy and chemical reaction effects on MHD mixed convection heat and mass transfer in a porous medium with thermal radiation and Ohmic heating. *Commun Nonlinear Sci Numer Simulat* , vol. 15, pp. 2878–2893.

Patil, P. R.; Rudraiah, N. (1973): Stability of hydromagnetic thermoconvective flowthrough porous medium. *Trans. ASME, J. Appl. Mech. E,* vol. 40, pp. 879–884.

Plappally A. K., Yakub I., Brown L. C., Soboyejo W. O.; Soboyejo A. B. O., (2009), Theoretical and Experimental Investigation of Water Flow through Porous Ceramic Clay Composite Water Filter, *FDMP: Fluid Dyn. Mater. Process*, vol. 5, no. 4, pp. 373-398.

Podolny A., Nepomnyashchy A.; Oron A., (2010), Rayleigh-Marangoni Instability of Binary Fluids with Small Lewis Number and Nano-Fluids in the Presence of the Soret Effect, *FDMP: Fluid Dyn. Mater. Process*, vol. 6, no. 1, pp. 13-40.

Rathish Kumar B.V.; Shalini (2005) Double diffusive natural convection in a doubly stratified wavy porous enclosure, *Applied Mathematics and Computation,* vol. 171, pp. 80–202.

Robillard, L. ; Bahloul, A.; Vasseur P. (2006). Hydromagnetic natural convection of a binary fluid in a vertical porous enclosure. *Chem. Eng. Comm.*, vol. 193, pp. 1431–1444.

Rouijaa H., El Alami M., El Alami Semma; Najam M., (2011), Natural Convection in an Inclined T-Shaped Cavity, *FDMP: Fluid Dyn. Mater. Process*, vol. 7, no. 1, pp. 57-70.

Rudraiah, N. (1984) Linear and non-linear magnetoconvection in a porous medium.

Proc. Indian Acad. Sci. (Math. Sci.), vol. 93, pp. 117–135.

Singh, A. K.; Thorpe G. R. (1995) Natural Convection in a Confined Fluid Overlying a Porous Layer – A Comparison Study of Different Models, *Indian J. Pure appl. Math*., vol. 26, no. 1, pp. 81-95.

Straughan, B. (2010): Structure of the dependence of Darcy and Forchheimer coefficients on porosity. *International Journal of Engineering Science,* vol. 48, no. 11, pp. 1610–1621.

Zhao, S.C.; Liu, Q.S. (2010): Thermal effects on Rayleigh–Marangoni–Bénard instability in a system of superposed fluid and porous layers, *International Journal of Heat and Mass Transfer,* vol. 53, pp. 2951–2954.